issn 0065-3713

INSTITUT D'AERONOMIE SPATIALE DE BELGIQUE

3 - Avenue Circulaire
B - 1180 BRUXELLES

AERONOMICA ACTA

A - N° 395 - 1996

Theoretical Plasma Distributions Consistent with Ulysses Magnetic Field Observations in a Solar Wind Tangential Discontinuity

by

J. De Keyser, M. Roth, J. Lemaire, B.T. Tsurutani, C.M. Ho and C.M. Hammond

BELGISCH INSTITUUT VOOR RUIMTE-AERONOMIE

3 - Ringlaan
B - 1180 BRUSSEL

FOREWORD

This paper has been accepted for publication in *Solar Physics.*

AVANT–PROPOS

Cet article a été accepté comme publication dans *Solar Physics.*

VOORWOORD

Dit artikel is aanvaard voor publikatie in *Solar Physics.*

VORWORT

Dieser Aufsatz wird in *Solar Physics* erscheinen.

Theoretical Plasma Distributions Consistent with Ulysses Magnetic Field Observations in a Solar Wind Tangential Discontinuity

J. De Keyser* M. Roth* J. Lemaire* B.T. Tsurutani§
C.M. Ho§ and C.M. Hammond¶

Abstract

The overall multi-layer structure of the magnetic field profile observed by ULYSSES across a broad solar wind tangential discontinuity can be reproduced fairly well by means of a kinetic model. Such a simulation provides complementary information about the velocity distribution functions, which are not always available from the plasma experiment due to the low time resolution inherent in plasma measurements. The success of such a simulation proves that the kinetic model can be used as a realistic basis for further studies of the structure and stability of solar wind tangential discontinuities.

Samenvatting

De meerlagige structuur van het magnetische veld profiel opgemeten door ULYSSES tijdens de doorgang doorheen een dikke tangentiële discontinuïteit in de zonnewind kan goed worden nagebootst door middel van een kinetisch model. Een dergelijke simulatie verschaft ons aanvullende informatie over de snelheidsverdelingsfuncties in het plasma; deze kan men niet altijd bekomen van de deeltjes-analysatoren omwille van de lage tijdsresolutie die eigen is aan dergelijke metingen. Het welslagen van de simulatie toont aan dat het gebruikte kinetische model een realistische basis vormt voor verdere studies van de structuur en de stabiliteit van tangentiële discontinuïteiten in de zonnewind.

*Belgian Institute for Space Aeronomy, Ringlaan 3, B-1180 Brussels, Belgium
§Jet Propulsion Lab., California Institute of Technology, Pasadena, CA 91109, U.S.A.
¶Los Alamos National Laboratory, Los Alamos, NM 87545, U.S.A.

Résumé

La structure globale, à couches multiples, d'un profil large du champ magnétique, observée par ULYSSES au travers d'une discontinuité tangentielle du vent solaire, peut être reproduite relativement bien à l'aide d'un modèle cinétique. Une telle simulation fournit des informations complémentaires sur les fonctions de distribution des vitesses ; en particulier, lorsque la résolution temporelle des instruments de plasma est faible. La réussite de pareille simulation démontre bien que le modèle peut être utilisé comme une base réaliste pour des études ultérieures de la structure et de la stabilité des discontinuités tangentielles du vent solaire.

Zusammenfassung

Die Struktur des Magnetfeldes beobachtet durch die ULYSSES Sonde in einer tangentiale Diskontinuität in dem Sonnenwind kan man ziemlich gut wiedergeben mittels eines kinetischen Modells. Diese Simulation gibt zusätzliche Information zu den Teilchengeschwindigkeitsverteilungsfunktionen. Diese Geschwindigkeitsverteilungen kan man nicht immer genau, durch die — typisch für Plasma Experimente — niedrige Beobachtungsfrequenz, bekommen. Die gute Ergebnisse von dieser Simulation zeigen das das vorliegende kinetische Modell eine realistische Basis ist für weitere Studien der Struktur und Stabilität von tangentialen Diskontinuitäten in dem Sonnenwind.

1. Introduction

Tangential discontinuities (TDs) are a prevalent feature of the solar wind (see e.g., (Burlaga *et al.*, 1977)). Results from ULYSSES indicate that TDs are common also at high heliographic latitudes (Tsurutani *et al.*, 1994). Solar wind TDs often exhibit different characteristic scales and are associated with shears in both the magnetic field and plasma velocity. A prerequisite for any theoretical study of TDs is a realistic model that is able to account for the overall internal structure observed in high time resolution magnetic field measurements. Kinetic TD models based on Vlasov equilibria (Lemaire and Burlaga, 1976; Lee and Kan, 1979; Roth *et al.*, 1993; Kuznetsova *et al.*, 1994; Kuznetsova and Roth, 1995) differ from each other by the analytical form of the velocity distribution function (VDF). They cannot account for the complex multiscale nature often present in solar wind TDs, as the number of free parameters in these models is reduced to a minimum (like in (Roth *et al.*, 1993) or (Kuznetsova and Roth, 1995)) depending on the specific application. In this paper a generalized model (that includes most previous models as special cases) using several species and parameterized VDFs (Roth *et al.*, 1996) is shown to be powerful enough to explain the overall magnetic field variation across a solar wind TD observed by ULYSSES. In the absence of plasma data with sufficient time resolution, such a simulation gives us some clues about the actual VDFs. The aim of this paper is not the study of this particular solar wind TD; rather, the emphasis is on the applicability of the model and its suitability as a basis for further theoretical investigation.

2. The kinetic TD model

The standard procedure for solving the Vlasov equations for charged particles (mass m and charge Ze) moving in a steady plane TD electromagnetic configuration (see e.g. (Longmire, 1963, chapter 5)) consists of first expressing the single-valued VDFs in terms of the constants of motion: the particle's energy H and canonical momenta $\mathbf{p} = (p_y, p_z)$ (x being the normal to the TD plane). In a second phase, the partial densities and currents are obtained as functions of the electrostatic potential $\phi(x)$ and the vector potential components $a_y(x)$ and $a_z(x)$, by integrating the VDFs over velocity space. Finally, Maxwell's equations lead to a set of coupled ordinary differential equations for $a_y(x)$ and $a_z(x)$, supplemented by the quasi-neutrality condition for $\phi(x)$. This set is solved numerically by means of an adaptive-step ODE integrator.

The fact that the particles from the left (right) side of the transition penetrate into the right (left) side over only a limited distance implies that their VDF must show an anisotropy. This anisotropy is reflected by the

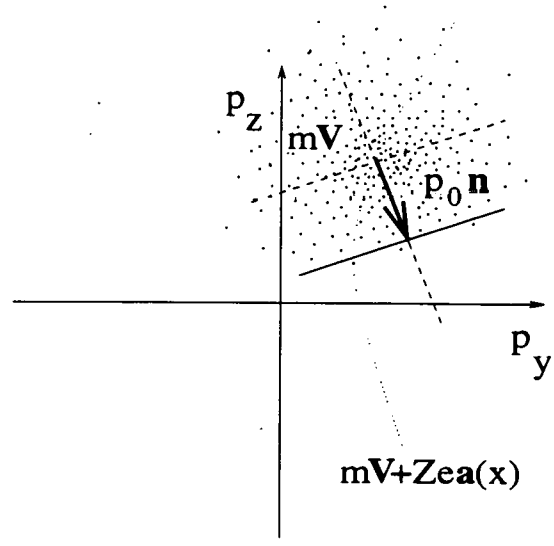

Fig. 1. Projection of the phase space onto the p_y, p_z plane at the center of the transition ($x = 0$, given the choice $\mathbf{a}(0) = \mathbf{0}$) for the case of protons. The population is characterized by a Maxwellian velocity distribution, modified by a cutoff to exclude particles in one half-space. The demarcation line is determined by its unit normal $\mathbf{n}$ and p_0; the sharpness of the cutoff depends on the characteristic length l. As x varies, the center of the distribution follows a trajectory determined by the magnetic potential $\mathbf{a}(x)$: when it lies further above the cutoff line, the population becomes purely Maxwellian, and when it moves to the opposite side of the demarcation line, the population density vanishes.

form of the VDF that is proposed: far from the transition the VDF is a pure Maxwellian, while the VDF is altered in the transition layer by a cutoff factor that demarcates a region in the phase space that is underpopulated. This is graphically illustrated in figure 1. The figure shows a projection of the phase space onto the p_y, p_z plane at the center of the transition ($x = 0$, given the choice $\mathbf{a}(0) = \mathbf{0}$ to fix the arbitrary constants in the definition of the magnetic potential) for the case of protons. The essentially Maxwellian distribution centered around an average tangential velocity $\mathbf{V}$ is modified by removing particles on one side of a given demarcation line. The VDF is expressed mathematically by:

$$F = \eta(H, \mathbf{p})G(U(\mathbf{p})),$$

where η is a Maxwellian at temperature T:

$$\eta = N(\frac{m}{2\pi kT})^{\frac{3}{2}} \exp(-\frac{H}{kT} - \frac{mV^2}{2kT} + \frac{p_y V_y + p_z V_z}{kT})$$

and G is a cutoff function ($C_1, C_2 \in [0, 1]$)

$$G = \frac{1}{2}\left[C_1 \operatorname{erfc}(-U(\mathbf{p})) + C_2 \operatorname{erfc}(U(\mathbf{p}))\right]$$

with $U(\mathbf{p}) = (\mathbf{p} - m\mathbf{V} - hp_0\mathbf{n}) \cdot \mathbf{n} \;/\; Ze\tilde{B}\rho\sqrt{l^2-1}$, where $\rho = \sqrt{2mkT}/|Z|e\tilde{B}$ is the gyroradius of the particle in a reference magnetic field $\tilde{B}$, and $h = \text{sign}\, Z$. The demarcation line has a direction determined by its unit normal $\mathbf{n}$; its position depends on p_0. The sharpness of the cutoff is specified by the transition length l (≥ 1), while the constants C_1 and C_2 determine which side of the demarcation line is underpopulated (Roth *et al.*, 1996). This formalism can also be used to describe populations of the Harris type (Harris, 1962): populations with bulk velocities ensuring that the particles remain confined within the transition layer, without requiring the introduction of a cutoff ($C_1 = C_2 = 1$).

3. Observations and simulation

Amongst the many TDs observed by ULYSSES we have selected one, observed on July 3, 1993, 5:29 UT, at 4.57 AU and $-33.8°$ heliographic latitude. Dashed lines on figure 2 show the magnetic field components in the minimum variance frame (MVF). This frame has additionally been rotated $-15°$ about the normal axis, such that the cutoff line in the simulation can be taken parallel to the p_y axis (i.e., $\mathbf{n} = \mathbf{1}_z$). The spacecraft velocity with respect to the Sun (a few km/s) is negligible compared to the high speed of the solar wind. MVF orientation and velocity data show the normal speed of ULYSSES relative to the TD plane to be 750 ± 10 km/s, implying a width of about 130000 km. This exceptional width (230 gyroradii of 21.5 eV protons in a 0.85 nT field) and the multiscale magnetic field variations indicate that this transition is composed of several current sheets. Solar wind TDs are known to have an average width of 36 ± 5 gyroradii (Lepping and Behannon, 1986), placing this particular TD among the widest ones.

We distinguish three parts in the magnetic field magnitude dip: the left and right inner regions (IL and IR, see figure 2) and a central inner depression (IC). The dip is bounded by two outer regions (OL and OR) defining the solar wind environment. Figure 2 shows that the transition consists of a B_z reversal, while B_y remains essentially constant; the magnetic field rotates over 90.6°. Experience with earlier kinetic models (Harris, 1962; Kuznetsova and Roth, 1995), shows that such a large rotation requires the presence of inner particle populations, i.e., populations with a density that decays rapidly with distance from the center of the transition.

The simulation relies on the high time resolution magnetometer data (1 vector/s), and plasma data from the ion spectrometer (that returns 3-dimensional spectra every 4 to 8 minutes) and the electron instrument (returning either 2- or 3-dimensional spectra every 5 to 11 minutes). Only solar wind properties near the right edge of the transition are available; there are no data close to the left edge, nor inside the transition. Because of the

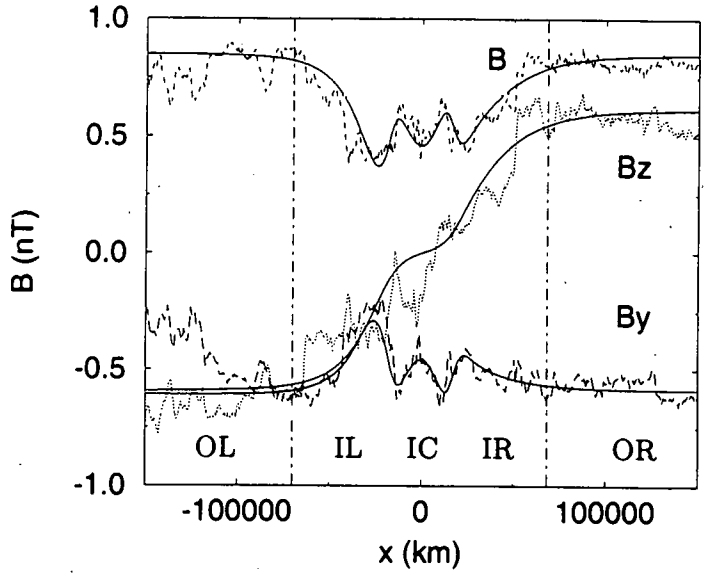

Fig. 2. Observed (dashed lines) and simulated (solid lines) magnetic field components in the MVF (rotated for convenience by $-15°$ along the x-axis). The average normal field (not shown) does not exceed 15 % of the field magnitude. The vertical lines delimit the TD crossing, centered at July 3, 5:29 UT, and lasting about 3 minutes. The horizontal axis gives the corresponding length scale along the TD normal. In the RTN-frame, the normal is $(0.957, -0.051, -0.298)$ and the proton velocity is $(781, -20, 6)$ km/s. This indicates that the TD was nearly orthogonal to the high speed solar wind flow direction.

symmetry in magnetic field intensity on both sides of the TD, it is reasonable to take equal plasma densities and temperatures for the outer regions. We also assume that the velocity shear between both outer plasmas can be neglected.

Table I gives the values of the VDF parameters that are able to account fairly well for the observed magnetic field profile. We have introduced 5 sets of populations. Each set consists of electrons of 4.4 eV, a proton population of 21.5 eV, and 100.0 eV alpha particles (the latter contribute significantly to the total current), according to the available plasma data. The particular choice of p_0 for the outer populations implies an overlap between them, defining a central plasma density enhancement of 12 %. This explains the central inner field depression. The asymmetry in the B_y component observed in the left and right inner depression, is explained in terms of the different z bulk velocities for the left and right inner populations. These inner populations also contribute to the B_z reversal through their drift velocities along y. To improve the fit even more, we have added a wide central inner population set.

TABLE I

Plasma populations used in the simulation.

	Z	m/m_p	$N(\mathrm{cm}^3)$	$T(\mathrm{eV})$	(V_y, V_z) (km/s)	(C_1, C_2)	l^* [a]	p_0^* [b]
outer	1	0.00055	0.3348	4.4	(0,0)	(0,1)	11	1.2
left	+1	1.00	0.3018	21.5	(0,0)	(0,1)	11	1.2
(OL)	+2	3.97	0.0165	100.0	(0,0)	(0,1)	11	1.2
inner	-1	0.00055	0.1540	4.4	(0.25,-0.34)	(0,1)	4.5	-15
left	+1	1.00	0.1400	21.5	(-1.22, 1.66)	(0,1)	4.5	-15
(IL)	+2	3.97	0.0070	100.0	(-5.68, 7.73)	(0,1)	4.5	-15
inner	-1	0.00055	0.0066	4.4	(0.25, 0)	(1,1)	-	-
center	+1	1.00	0.0060	21.5	(-1.22, 0)	(1,1)	-	-
(IC)	+2	3.97	0.0003	100.0	(-5.68, 0)	(1,1)	-	-
inner	-1	0.00055	0.0550	4.4	(0.25, 0.10)	(1,0)	4.0	14
right	+1	1.00	0.0500	21.5	(-1.22,-0.49)	(1,0)	4.0	14
(IR)	+2	3.97	0.0025	100.0	(-5.68,-2.27)	(1,0)	4.0	14
outer	-1	0.00055	0.3348	4.4	(0,0)	(1,0)	11	-1.2
right	+1	1.00	0.3018	21.5	(0,0)	(1,0)	11	-1.2
(OR)	+2	3.97	0.0165	100.0	(0,0)	(1,0)	11	-1.2

[a]: $l^* = l\rho/\tilde{\rho}$ where $\tilde{\rho}$ is the 20 eV proton gyroradius in a 1 nT magnetic field (650 km)
[b]: $p_0^* = p_0/\tilde{p}$ where $\tilde{p}$ is the thermal momentum of 20 eV protons (10^{-22} kg · m / s)

Figure 2 compares the simulated magnetic field (solid lines) with the observations (dashed lines), showing the good fit of the overall magnetic field profile. The fine wavy-like structure superimposed on it cannot be reproduced. It may be ascribed to the propagation of waves across the TD. Alternatively, the TD might be in a state of turbulence (Kuznetsova *et al.*, 1995). Nevertheless, the equilibrium model can serve as a first approximation; it can be used to describe the unperturbed state in a subsequent study of TD instabilities.

The electron densities, shown in figure 3, illustrate the role of the populations in each region. Note in particular the central density enhancement due to the overlap between both outer populations.

4. Discussion

In this paper we have used a generalized Vlasov model of TDs. We have obtained a "best choice" for the VDF parameters that mimics a TD magnetic field profile recorded by ULYSSES. Previously, only hypothetical solar wind

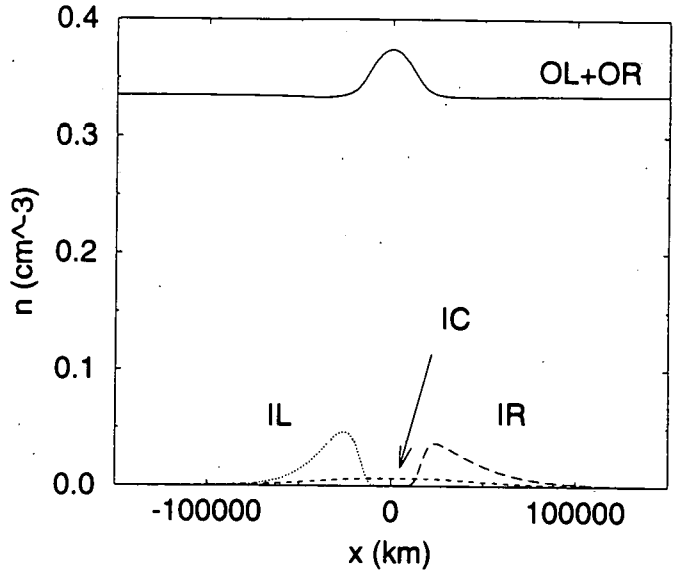

Fig. 3. Calculated electron densities using the VDFs from table I. Note the central density enhancement, and the IL and IR current layers interfacing it with the outer plasma environment.

TDs have been simulated with Vlasov models (Lemaire and Burlaga, 1976; Roth, 1986); here, we model an actually observed event. In the absence of high time resolution plasma data, the simulation gives important clues about the nature of the actual VDFs. For instance, inner populations with different bulk velocities have to be postulated to account for the observed magnetic field rotation. The multi-layer structure of the transition is controlled by the length scales and separation (or overlap) of the populations.

This TD simulated here is quite wide and represents a piling up of several current layers: it is a denser plasma region, separated from the surrounding solar wind by a current sheet on either side (with current densities of the order of 3.10^{-11} A/m^2). In general, simulations like the one performed here offer the possibility of computing quantities which are not directly observable, such as the electric field strength. For instance, in this particular simulation we have obtained electrostatic potential variations of less than 50 mV, corresponding to an extremely weak electric field along the TD normal. Its precise value is of no particular interest; what matters is that an equilibrium electric field exists as a natural consequence of the tendency of a plasma to remain neutral. Still, it plays an important role in the study of magnetic field line stochasticity and particle diffusion in electrostatically non-equipotential TDs (Kuznetsova and Roth, 1995).

The successful simulation demonstrates the ability of the kinetic model to describe the overall characteristics of observed magnetic field profiles. Therefore, it can serve as a basic model for further studies of TD related phenomena. For instance, the wave-like structure of the small-scale magnetic field variations can be analyzed by looking at the difference between the equilibrium model and the high resolution observations. The power spectrum of the difference can provide insight into possibly excited instabilities and their preferred wavelengths.

Several intrinsic limitations of the one-dimensional, time-independent Vlasov approach should be kept in mind. In particular, Vlasov theories of plane TDs employ nonunique distribution functions and do not address the problem of particle accessibility (Whipple *et al.*, 1984). Moreover, current layers with large magnetic or velocity shear, density and temperature gradients, are thermodynamically nonequilibrium systems that have an excess of free energy and are potentially unstable with respect to the excitation of large scale electromagnetic perturbations (Kuznetsova *et al.*, 1995). Therefore, TDs most likely are in a state of turbulence rather than in a state of equilibrium. Kuznetsova *et al.* (1995) have proposed a method which reduces the arbitrariness in the Vlasov formulation: the optimal choice for the free parameters of the model is the one leading to the most stable configuration that satisfies the boundary conditions.

In order to study the time evolution of TDs, one can adopt a realistic 1D equilibrium model, like the one presented here, as an initial state, and consider the effects of superposed perturbations. This introduces 3D effects in the model in the form of small-amplitude long-wavelength variations of fields in the plane of the current sheet. As an alternative, hybrid particle simulations that use an ensemble of ion particles immersed in an electron fluid (e.g., Omidi and Winske, 1995) can trace the evolution of TDs. Electron inertia, however, plays a critical role in configurations with large magnetic shear and cannot be adequately described by present particle simulation codes, mainly because of limited computational resources.

5. Acknowledgements

The authors thank A. Balogh (Imperial College, London, England) for providing the magnetic field data, and J.L. Phillips (Los Alamos National Laboratory, NM) for the plasma data. They also thank M.M. Kuznetsova for fruitful discussions. J.D.K., M.R. and J.L. are supported by the ESA (PRODEX) project "Interdisciplinary Study of Directional Discontinuities" as part of the ULYSSES mission, and acknowledge the support of the Belgian Federal Services for Scientific, Technological and Cultural Affairs. The research by B.T. and C.H. was carried out at the Jet Propulsion Labora-

tory, California Institute of Technology, under a contract with the National Aeronautics and Space Administration (USA).

References

Burlaga, L.F., Lemaire, J.F., and Turner, J.M.: 1977, *J. Geophys. Res.* **82**, 3191.
Harris, E.G.: 1962, *Nuovo Cimento* **23**, 115.
Kuznetsova, M.M., and Roth, M.: 1995, *J. Geophys. Res.* **100**, 155.
Kuznetsova, M.M., Roth, M., Wang, Z., and Ashour-Abdalla, M.: 1994, *J. Geophys. Res.* **99**, 4095.
Kuznetsova, M.M., Roth, M., and Zelenyi, L.M.: 1995, in P. Song, B.U.Ö. Sonnerup, and M.F. Thomsen, ed(s)., *Physics of the magnetopause, Geophys. Monogr. Ser., vol. 90*, AGU, Washington, D.C., 99–108.
Lee, L.C., and Kan, J.R.: 1979, *J. Geophys. Res.* **84**, 6417.
Lemaire, J., and Burlaga, L.F.: 1976, *Astrophys. Space Sci.* **45**, 303.
Lepping, R.P., and Behannon, K.W.: 1986, *J. Geophys. Res.* **91**, 8725–8741.
Longmire, C.L.: 1963, Interscience Publishers: New York.
Omidi, N., and Winske, D.: 1995, *J. Geophys. Res.* **100**, 11935.
Roth, M.: 1986, in R.G. Marsden, ed(s)., *The Sun and the Heliosphere in Three Dimensions, ASSL123*, D. Reidel Publ. Co., Dordrecht, 167–171.
Roth, M., De Keyser, J., and Kuznetsova, M.M.: 1996, *Space Science Rev.* , In press.
Roth, M., Evans, D.S., and Lemaire, J.: 1993, *J. Geophys. Res.* **98**, 411.
Tsurutani, B.T., Ho, C.M., Smith, E.J., Neugebauer, M., Goldstein, B.E., Mok, J.S., Arballo, J.K., Balogh, A., Southwood, D.J., and Feldman, W.C.: 1994, *Geophys. Res. Lett.* **21**, 2267–2270.
Whipple, E.C., Hill, J.R., and Nichols, J.D.: 1984, *J. Geophys. Res.* **89**, 1508–1516.